Supplementary Material: Spin Amplification for Magnetic Sensors Employing Crystal Defects

Marcus Schaffry,[1] Erik M. Gauger,[1,2] John J. L. Morton,[1,3] and Simon C. Benjamin[1,2]

[1]Department of Materials, University of Oxford, Parks Road, Oxford OX1 3PH, United Kingdom
[2]Centre for Quantum Technologies, National University of Singapore, 3 Science Drive 2, Singapore 117543
[3]Clarendon Laboratory, University of Oxford, Parks Road, OX1 3PU, United Kingdom

(Dated: August 31, 2011)

In this Supplementary Material, we first derive an expression for the sensitivity of a single spin. Next, we give a detailed analysis of different measurement strategies for reading out the NV centre spin with respect to the ratio S_{NV}/S_A. In particular, we show that reliable single shot readout is not a requirement for realising the advantage of our proposed scheme over the conventional sensor proposal. Finally, we briefly discuss the consequences of an imperfect π-pulse in the amplifier spin scheme.

SENSITIVITY OF A SINGLE SPIN

We begin with a general discussion of measuring an unknown magnetic field using two energy levels of a probe spin s system ($2s \in \mathbb{N}$), the underlying principle of the NV centre sensor. Let the probe spin be governed by the Zeeman Hamiltonian $H = -\mu_{\mathrm{Prb}}(B_0 + B)S_z$, where μ_{Prb} is the magnetic moment of the probe spin, S_z is the usual spin operator, B_0 is a known external field applied in the z-direction, and B corresponds to the magnetic field (also in the z-direction) that we wish to estimate. Consider two eigenstates $|0\rangle$ and $|1\rangle$ of H whose z-projections differ by an integer m. The field estimation then proceeds as follows: we start by creating the superposition $|+\rangle$ [here $|\pm\rangle = 1/\sqrt{2}(|0\rangle \pm |1\rangle)$], for example by using a suitable microwave or radio-frequency pulse sequence. This state evolves in time to $|\psi(t)\rangle = 1/\sqrt{2}(|0\rangle + \exp(im\mu_{\mathrm{Prb}}(B_0+B)t/\hbar)|1\rangle)$ and therefore by successive measurements of the spin, we can infer the strength of the magnetic field. In any real-world experiment the state $|\psi(t)\rangle$ will also be affected by decoherence processes, typically dephasing is predominant [1]. In this case, the coherence between $|0\rangle$ and $|1\rangle$ decays as $\exp(-\gamma(t))$ for a positive non-decreasing function $\gamma(t)$. The time evolution of the two level system's density matrix $\rho(t)$ is then fully described by

$$\rho(t) = \frac{1}{2}\begin{pmatrix} 1 & e^{i\frac{m\mu_{\mathrm{Prb}}(B_0+B)}{\hbar}t-\gamma(t)} \\ e^{-i\frac{m\mu_{\mathrm{Prb}}(B_0+B)}{\hbar}t-\gamma(t)} & 1 \end{pmatrix} \quad . \tag{1}$$

The uncertainty of estimating B is limited by the quantum Cramér-Rao bound (CRB), i.e. even for an ideal system and perfect measurements the uncertainty in δB cannot become smaller than b_{CR}. The CRB is given by the inverse square root of the quantum Fisher information F with respect to B [2, 3], yielding the following inequality

$$\delta B \geq b_{\mathrm{CR}} = \frac{1}{\sqrt{F}} = \frac{e^{\gamma(\tau)}\hbar}{m\tau|\mu_{\mathrm{Prb}}|} \quad , \tag{2}$$

where τ is the duration for which the spin has experienced the magnetic field. Repeating the measurement many times gives a further reduction in the uncertainty of the unknown field. Assuming the preparation of the $|+\rangle$ state takes the time t_p, the lower bound for the uncertainty δB after $N = T/(\tau + t_p)$ repetitions within a total time T is given by

$$b_{\mathrm{CR}} = \frac{1}{\sqrt{NF}} = \frac{e^{\gamma(\tau)}\hbar\sqrt{\tau + t_p}}{\sqrt{T}m\tau|\mu_{\mathrm{Prb}}|} \quad . \tag{3}$$

As an example, we set $\gamma(t) = \frac{t}{T_2}$. It is easily seen that the optimal sensing time for each run of the protocol is $\tau^* \approx \frac{1}{2}T_2$ in the limit of weak dephasing ($T_2 \gg t_p$), in contrast to $\tau^* \approx T_2$ when the dephasing time is comparatively short, $T_2 \ll t_p$.

READOUT OF THE NV CENTRE SPIN

The readout of the NV centre spin can be implemented in several ways and we here discuss the three most relevant and practical possibilities. Importantly, we will show that imperfect measurements affect the conventional and the amplified sensor in a similar way. As a consequence the advantage conveyed by the amplifier spin is not conditional on the measurement fidelity.

Non-resonant readout of the NV centre spin

At room-temperature the readout of the NV centre spin is typically performed by non-resonant optical excitation [4, 5]. Both the $|0\rangle$ and the $|\pm 1\rangle$ levels are simultaneously excited by a green laser pulse. The measurement consists of detecting a small difference in the fluorescence brightness between the different optical transitions. However, after about 0.5 µs the laser illumination polarizes the NV centre spin by pumping it into the $|0\rangle$ state. Hence, there is only a small time window for spin-dependent fluorescence photon detection before the original spin state is destroyed. Moreover, the vast majority of photons emitted is lost in typical experimental settings.

For the traditional NV centre sensing scheme this implies that we need to repeat the measurement many times to detect a sufficient number of photons to allow any inferences about the spin state of the NV centre. We can account for this photon-shot noise limitation by modifying the magnetic moment sensitivity given in Eq. (4) of the main article as $S_{\mathrm{off}} = S/(R\sqrt{\eta})$, where R is the measurement contrast and η is the detection efficiency [6, 7]. Recent experiments with single NV centres found values of $R \approx 0.2$ and $\eta \approx 0.001$ [4, 8, 9]. However, with a tapered fibre or a plasmonic waveguide the detector efficiency could be improved to about $\eta = 0.05$ [10].

To achieve a fair comparison we assume the same readout procedure for both sensing methods, the traditional NV centre sensor and our amplified sensor proposal. In the latter case this entails that the initialisation process needs to be repeated $1/(R^2\eta)$ times to prepare a known initial state. Further, the readout of the amplifier spin after the sensing also takes about $1/(R^2\eta)$ times longer than in the ideal single shot readout case. In this case the measurement is performed by repeatedly mapping the amplifier spin state onto the NV centre spin with a selective π-pulse, followed by imperfect measurements of the NV centre spin (analogously to [11]). In summary we find that the preparation time for this method is given by $t_{p,\mathrm{A}} = \frac{1}{R^2\eta}(t_{p,\mathrm{NV}} + \tau_\pi)$ and the magnetic moment sensitivity is given as in Eq. (4) of the main text. Here, we have assumed that the T_1 of the amplifier spin is much longer than $t_{p,\mathrm{A}}$. In Fig. 1 we plot $t_{p,\mathrm{A}}$ as a function of the dephasing time of the NV centre $T_{2,\mathrm{NV}}$.

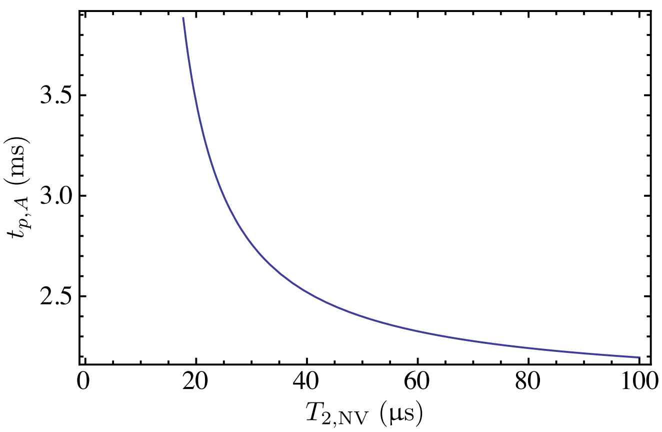

FIG. 1. (Color online) Preparation time necessary for the amplifier spin NV centre sensor with respect to the dephasing time of the NV centre $T_{2,\mathrm{NV}}$. Parameters: $t_{p,\mathrm{NV}} = 1$ μs, $R = 0.2$, $\eta = 0.05$ and $\Delta =$ 10 nm.

For the ratio of the magnetic moment sensitivity of both methods we obtain

$$\frac{S_{\mathrm{NV}}}{S_A} = \frac{1}{R\sqrt{\eta}} \frac{\exp(\gamma_{\mathrm{NV}}(\tau^*_{\mathrm{NV}}))\sqrt{\tau^*_{\mathrm{NV}} + t_{p,\mathrm{NV}}}\,\tau^*_A}{\exp(\gamma_A(\tau^*_A))\sqrt{\tau^*_A + t_{p,A}}\,\tau^*_{\mathrm{NV}}} \frac{r^3_{\mathrm{NV}}}{r^3_A} \quad , \quad (4)$$

which we plot in Fig. 4 of the main article.

As in the main text we assume the same dephasing mechanism for the NV centre and the amplifier spin. We consider the three cases $\gamma_i(t) = \left(\frac{t}{T_2}\right)^i$ for $i = 1,2,3$. By assuming that $t_{p,A} \gg T_{2,A}$ and $t_{p,\mathrm{NV}} \ll T_{2,\mathrm{NV}}$ we find that the optimal sensing times in Eq. (4) of the main text are given by $\tau^*_{A,1} = T_{2,A}$, $\tau^*_{A,2} = \frac{1}{\sqrt{2}}T_{2,A}$ and $\tau^*_{A,3} = 3^{-1/3}T_{2,A}$ and $\tau^*_{\mathrm{NV},1} = \frac{1}{2}T_{2,\mathrm{NV}}$, $\tau^*_{\mathrm{NV},2} = \frac{1}{2}T_{2,\mathrm{NV}}$ and $\tau^*_{\mathrm{NV},3} = 6^{-1/3}T_{2,\mathrm{NV}}$, where the index $i = 1,2,3$ labels which of the γ_i is used as the dephasing model. Under these assumptions, we can derive an approximation for the ratio in Eq. (4)

$$\frac{S_{\mathrm{NV}}}{S_A} \approx C_i \frac{T_{2,A}}{\sqrt{T_{2,\mathrm{NV}}}\sqrt{t_{p,\mathrm{NV}} + \tau_\pi}} \frac{r^3_{\mathrm{NV}}}{r^3_A} \quad , \quad (5)$$

where only the prefactor depends on the choice of the dephasing model as follows: $C_1 = \sqrt{2/e}$, $C_2 = e^{-1/4}$ and $C_3 = \left(\frac{2}{3e}\right)^{1/6}$. Interestingly, this ratio does not depend on the measurement contrast R nor the detector efficiency η. This means that both strategies are affected by the imperfect measurement in the same way.

Resonant readout of the NV centre spin

At low temperatures the $|0\rangle$ state can be excited resonantly (selectively) enabling single shot readout. The resonant excitation takes about 5 ms [12], which of course implies that the T_1 time of the NV centre spin needs to be longer than this time. We plot the ratio for this case, which is

$$\frac{S_{\mathrm{NV}}}{S_A} = \frac{\exp(\gamma_{\mathrm{NV}}(\tau^*_{\mathrm{NV}}))\sqrt{\tau^*_{\mathrm{NV}} + t_{p,\mathrm{NV}}}\,\tau^*_A}{\exp(\gamma_A(\tau^*_A))\sqrt{\tau^*_A + t_{p,A}}\,\tau^*_{\mathrm{NV}}} \frac{r^3_{\mathrm{NV}}}{r^3_A} \quad (6)$$

in Fig. 2.

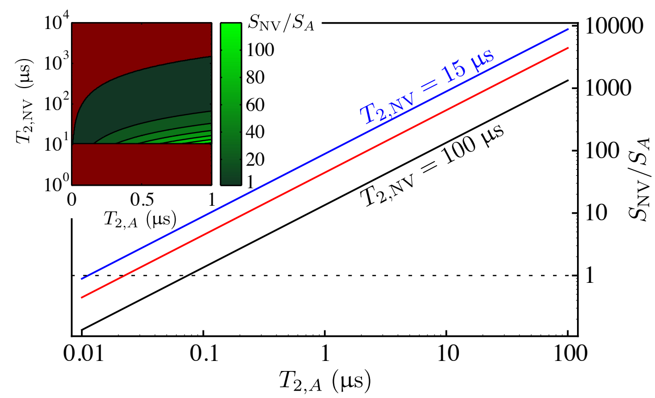

FIG. 2. (Color online) Resonant readout of the NV centre spin. Main plot: the ratio S_{NV}/S_A as a function of the amplifier spin coherence time $T_{2,\mathrm{A}}$ for $T_{2,\mathrm{NV}} = 100$ μs (black), 30 μs (red), and 15 μs (blue). This ratio gives the factor by which the amplified sensor outperforms a conventional NV centre sensor. Here $\gamma(t) = t/T_2$, but we note that the curves for $\gamma(t) = (t/T_2)^{2,3}$ look almost identical. Parameters: $t_{p,\mathrm{NV}} = 5$ ms, $t_{p,\mathrm{A}} = t_{p,\mathrm{NV}} + \tau_\pi$ $r_A = 1$ nm, $r_{\mathrm{NV}} = 11$ nm, $\Delta = 10$ nm. Inset: excessive line-broadening or a significant mismatch in the coherence times prevent a sensitivity enhancement in the red region (see main article).

Again we can find an approximation for the ratio in Eq. (6). As $t_{p,\mathrm{NV}} \approx 5$ ms it holds that $t_{p,\mathrm{NV}/A} \gg T_{2,\mathrm{NV}/A}$, yielding

$$\frac{S_{\mathrm{NV}}}{S_A} \approx \frac{T_{2,A}}{T_{2,\mathrm{NV}}} \frac{r^3_{\mathrm{NV}}}{r^3_A} \sqrt{\frac{t_{p,\mathrm{NV}}}{t_{p,A}}} = \frac{T_{2,A}}{T_{2,\mathrm{NV}}} \frac{r^3_{\mathrm{NV}}}{r^3_A} \sqrt{\frac{t_{p,\mathrm{NV}}}{t_{p,\mathrm{NV}} + \tau_\pi}} \quad , \quad (7)$$

which is entirely independent of the choice of $\gamma_i(t)$.

Readout using a local memory

A third way of reading out the electron spin of the NV centre is given by employing a nuclear spin (with a long T_1 time) in the immediate vicinity of the NV centre as a temporary memory. The amplifier spin state is here transfered to this nuclear spin, e.g. via the NV centre electron spin. This can also be accomplished at room temperature. A projective measurement is now possible using a quantum non-demolition scheme in the way described by Ref. [11]. Like in the previous section $t_{p,\mathrm{NV}} \approx 5$ ms and we thus obtain similar results.

IMPERFECT π-PULSE

Here, we briefly outline the consequences of an imperfect π-pulse for implementing the CNOT-gate between the amplifier and the NV centre electron spin. In general, a reduced π-pulse selectivity gives rise to two types of error: firstly, a mixed initial state, resulting in a correction factor of $(1+p)/(1-p)$ for the sensitivity S_A, where p describes the proportion of the population flipped in the unwanted transition. Secondly, a degradation of the Fisher information entailing an additional correction factor of $\sqrt{(1+p)/(1-p)}$. Both factors are very close to 1 as long as the pulse remains highly selective.

[1] A. Shaji and C. M. Caves, Phys. Rev. A **76**, 032111 (2007).
[2] S. L. Braunstein and C. M. Caves, Phys. Rev. Lett. **72**, 3439 (1994).
[3] M. G. A. Paris, Int. J. Quant. Inf. **7**, 125 (2009).
[4] J. R. Maze, P. L. Stanwix, J. S. Hodges, S. Hong, J. M. Taylor, P. Cappellaro, L. Jiang, M. V. G. Dutt, E. Togan, A. S. Zibrov, A. Yacoby, R. L. Walsworth, and M. D. Lukin, Nature **455**, 644 (2008).
[5] J. M. Taylor, P. Cappellaro, L. Childress, L. Jiang, D. Budker, P. R. Hemmer, A. Yacoby, R. Walsworth, and M. D. Lukin, Nature Physics **4**, 810 (2008).
[6] V. M. Acosta, E. Bauch, M. P. Ledbetter, C. Santori, K.-M. C. Fu, P. E. Barclay, R. G. Beausoleil, H. Linget, J. F. Roch, F. Treussart, S. Chemerisov, W. Gawlik, and D. Budker, Phys. Rev. B **80**, 115202 (2009).
[7] V. M. Acosta, E. Bauch, A. Jarmola, L. J. Zipp, M. P. Ledbetter, and D. Budker, Appl. Phys. Lett. **97**, 174104 (2010).
[8] G. Balasubramanian, P. Neumann, D. Twitchen, M. Markham, R. Kolesov, N. Mizuochi, J. Isoya, J. Achard, J. Beck, J. Tissler, V. Jacques, P. R. Hemmer, F. Jelezko, and J. Wrachtrup, Nat. Mater. **8**, 383 (2009).
[9] G. Balasubramanian, I. Y. Chan, R. Kolesov, M. Al-Hmoud, J. Tisler, C. Shin, C. Kim, A. Wojcik, P. R. Hemmer, A. Krueger, T. Hanke, A. Leitenstorfer, R. Bratschitsch, F. Jelezko, and J. Wrachtrup, Nature **455**, 648 (2008).
[10] D. E. Chang, A. S. Sørensen, P. R. Hemmer, and M. D. Lukin, Phys. Rev. Lett. **97**, 053002 (2006).
[11] P. Neumann, J. Beck, M. Steiner, F. Rempp, H. Fedder, P. R. Hemmer, J. Wrachtrup, and F. Jelezko, Science **329**, 542 (2010).
[12] J. Wrachtrup and F. Jelezko, J. Phys.: Condens. Matter **18**, S807 (2006).